

DNA photolyase of enterococci: possible explanation for its low sunlight inactivation rate

Mushtaq HUSSAIN^{1,2}, Syeda QAMARUNNISSA³, Saboohi RAZA⁴, Javed QURESHI³, Abdul WAJID⁵ & Sheikh A. RASOOL^{1*}

¹Department of Microbiology, University of Karachi, University Road, 75270-Karachi, Pakistan; email: ajazrasool@hotmail.com

²Department of Microbiology and Pathology, Aga Khan University, Pakistan

³Institute of Biotechnology and Genetic Engineering (KIBGE), University of Karachi, Pakistan

⁴Nuclear Institute of Agriculture, Tandojam, PAEC, Pakistan

⁵HEJ Research Institute of Chemistry, University of Karachi, Karachi, Pakistan

Abstract: DNA photolyase is perhaps the most ancient and direct arsenal in curing the UV-induced dimers formed in the microbial genome. Out of two cofactors of the enzyme, catalytic and light harvesting, differences in the latter have provided basis for categorizing photolyases of prokaryotes as folate and deazaflavin types. In the present study, the homology modeling of DNA photolyase of *Enterococcus faecalis* was undertaken. The predicted models were structurally compared with the crystal structure coordinates of photolyases from *Escherichia coli* (folate type) and *Anacystis nidulans* (deazaflavin type). Discrepancies present in the multiple sequence alignment and tertiary structures, particularly at the light harvesting cofactor (methenyltetrahydrofolic acid, MTHF; 8-hydroxy-5-deazaflavin, 8-HDF) binding sites indicated the mechanistic nature of enterococcal photolyase. Concisely, despite the greater holistic homology with folate-type photolyase, enterococcal photolyase was characterized as deazaflavin-type. The presence of 8-HDF binding sites and groove architecture of substrate binding sites were also found supportive in this regard. The inter cofactor distance and/or orientation also implied to the efficient energy transfer in photolyase of *Enterococcus* in comparison with *E. coli*. In addition, we observed relatively high protein deformability in the enterococcal genome, which may favor the repair action of photolyase. The findings are expected to provide molecular insights into the difference in sunlight inactivation rate of two important fecal contamination indicators, namely *Enterococcus* and *E. coli*.

Key words: *Enterococcus*; DNA-photolyase; pyrimidine dimers; sunlight inactivation; fecal contamination indicator.

Abbreviations: CPD, cyclobutane pyrimidine dimer; FAD, flavin adenine dinucleotide; 8-HDF, 8-hydroxy-5-deazaflavin; LHC, light harvesting cofactor; MTHF, 5,10-methenyltetrahydrofolic acid; P1, *Enterococcus faecalis* photolyase; P2, *Escherichia coli* photolyase; P3, *Anacystis nidulans* photolyase.

Introduction

Photoreactivation is considered to be the most direct mechanism to reverse the UV-induced DNA lesions among bacteria. Sunlight UV irradiation (260–320 nm) induces formation of *cis-syn* cyclobutane pyrimidine dimer (CPD), pyrimidine (6–4) pyrimidone photo-products (6–4PPs, pyrimidine adducts) and their Dewar valence isomers (Clingen et al. 1995; Yoon et al. 2000). Around 80–90% of all photo lesions are CPDs that consequently lead to cell death by blocking the all important biosynthesis of nucleic acid. The lethal manifestations of CPDs could be averted by the action of monomeric photoreactive flavoprotein of ~450 residues, namely DNA-photolyase (Sancar 2003; Zhong et al. 2007). Based on the amino acid sequence homology photolyases are classified into two types, I and

II, which are, respectively, common among prokaryotes and higher eukaryotes (Kato et al. 1994; Yasui et al. 1994). Intriguingly, presence of strong structural similarities (from primary to tertiary level) is not extended to their functionality; as the former is involved in DNA repair while the latter (cryptochromes) is important in photomorphogenesis, phototropism and circadian photoreception (Cashmore et al. 1999; Sancar 2003).

DNA photolyase (Class-I) contains two cofactors/chromophores, catalytic and light harvesting cofactor (LHC). Reduced flavin adenine dinucleotide (FAD) acts as the catalytic cofactor and it transfers the electron to CPDs and restores the original conformation of the bases. LHC acts as an antenna to harvest light energy and subsequently transfers it to the catalytic cofactor. Based on chemical nature, LHCs of class I photolyases have been categorized into two types,

* Corresponding author

namely folate and deazaflavin type. The LHC of folate-type photolyase is 5,10-methenyltetrahydrofolic acid (MTHF) (Johnson et al. 1988). Conversely, deazaflavin-type photolyase bears 8-hydroxy-5-deazaflavin (8-HDF) as LHC (Eker et al. 1990). Briefly, the photoreactivation initiates with the binding of enzyme with the DNA and flipping the dimer out of the double helix (Berg & Sancar 1998). This follows with the absorption of light photons (350–450 nm) by LHC and subsequent transfer of excitation energy (in the form of electron) to flavin via dipole-dipole interaction (Kim et al. 1991, 1992; Carell et al. 2001; Zhong et al. 2007). The flavin (excited) ultimately transfers an electron to dimer and renders separation of bases; concomitantly the electron is transferred back to nascent flavin to regenerate its reduced form for any impending catalytic activity (Epple & Carell 1998; Sancar 2003; Harrison et al. 2005). In this connection, the comparison of crystal structures of *Escherichia coli* photolyase (folate-type) and *Anacystis nidulans* (deazaflavin-type) has illustrated many functional similarities and dissimilarities between the two (Park et al. 1995; Tamada et al. 1997).

Sunlight (UV irradiation) rendered lethality (inactivation) has been reported as most important mechanism of inactivating sewage microorganisms including fecal contamination indicators (Davies-Colley et al. 1994; Sinton et al. 1999; Hussain et al. 2007). Moreover, sunlight inactivation rate of coliforms has also been found higher in comparison to enterococci. The difference in susceptibility has been attributed to intrinsic susceptibility of both indicators to different solar wavelength and penetration of these wavelengths in contaminated water (Sinton et al. 2002). This has reportedly provided advantage to enterococci over *E. coli* to be exploited as fecal contamination indicator (Sinton et al. 1999, 2002; Hussain et al. 2007).

In the present study we have tried to unravel the nature of DNA photolyase of *Enterococcus faecalis* (most abundant enterococci in sewage) and its comparison has been undertaken with photolyase of *E. coli* (a major component of coliforms) and *A. nidulans* (template). It is believed that the findings will help in the molecular understanding of low sunlight inactivation of *E. faecalis* as compared to *E. coli* on the bases of structure-activity relationships of DNA photolyases. Additionally, it may also provide a model to explicate difference in UV susceptibility among different microorganisms. To the best of our knowledge, this is the first report on structure-activity relationships of enterococcal photolyase.

Methods

Multiple sequence alignment

Amino acid sequences of DNA photolyase from *E. faecalis* V583 (accession No. NP_815313), *E. coli* (NP_415326) and *A. nidulans* (YP_399131) were retrieved from NCBI (National Center for Biotechnology Information) data bank (Wheeler et al. 2005). The program FASTA and BLAST tool (Altschul et al. 1997) were used to retrieve the primary and

tertiary structure homologues of enterococcal photolyase. Multiple sequence alignment was generated by default parameters of program ClustalX (Thomson et al. 1997). The alignment file was analyzed using the program GeneDoc (Nicholas et al. 1997) and visualized by CLC Sequence viewer 6.0.2. (<http://www.clcbio.com/index.php?id=28>).

Homology modeling

The atomic coordinates of DNA photolyase of *E. coli* (PDB code 1DNPA) (Park et al. 1995) and *A. nidulans* (1OWLA) (Tamada et al. 1997) were obtained from Protein Data Bank (Berman et al. 2000). The three-dimensional model of enterococcal photolyase was developed using the crystal structure coordinates of *A. nidulans* photolyase (Tamada et al. 1997) using 3D-JIGSAW (Bates et al. 2001) and SWISS-MODEL (Schwede et al. 2003) with manual input of PDB code.

Tertiary structure analysis

The structural coordinates of enterococcal photolyase were viewed by Swiss-PDB viewer (Guex et al. 1997) and Accelrys Discovery Studio Visualizer 2.0 (<http://accelrys.com/products/discovery-studio/>). All models were analyzed for structural and thermodynamic stability using Swiss-PDB viewer, PROCHECK, Whatcheck (Laskowski & Kato 1980), ANOLEA (Melo & Feytman 1998) and Verify3D (Elsenberg et al. 1997). Fold recognition was performed by 3D-PSSM algorithm (Kelley et al. 2000).

Protein deformability of genome

Extent of protein-induced genomic deformability of *E. faecium* and *E. coli* was established by method of Worning et al. (2001) and retrieved from Center for Biological Sequence Analysis (<http://www.cbs.dtu.dk/services/GenomeAtlas/>) (Hallin & Ussery 2004).

Results and discussion

Sequence analysis

Multiple sequence alignment of enterococcal photolyase exhibited 52% and 48% of sequence similarity with photolyase of *E. coli* and *A. nidulans*, respectively. For the sake of brevity, in the most parts of following script we have abbreviated *E. faecalis* photolyase as P1 and photolyase from *E. coli* and *A. nidulans* as P2 and P3, respectively. The sequence homology was found more conspicuous towards the C-termini of the enzymes suggesting the common role of the region in all types of photolyases, i.e. folate- and deazaflavin-type (Fig. 1). Indeed, it is known that the binding sites of common catalytic cofactor (FAD) are mainly situated within C-terminal of the proteins (Park et al. 1995; Tamada et al. 1997; Komori et al. 2001). This notion was further intensified by closer comparison of FAD-binding residues in the sequence alignment. In this regard, Tyr219, Thr230, Ser231, Leu233, Arg270, Trp328, Asp362, Asp364 and Asn368 of P1 were found in both folate-type (P2) and deazaflavin-type (P1 and P3) almost at the same corresponding position. The minor discrepancy in FAD-binding sites was noticed, as Phe263 is present in P1 instead of iso-functional tryptophan at the corresponding position in other two analyzed sequences (P2 and P3). More

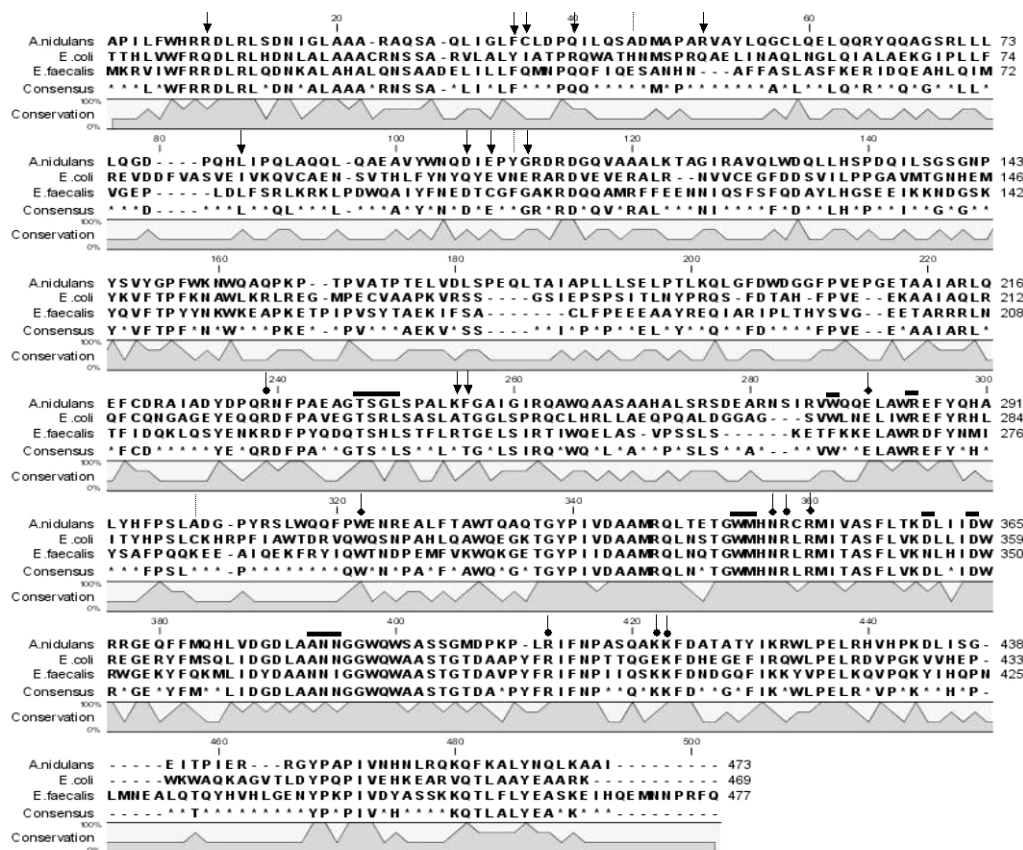


Fig. 1. Multiple sequence alignment of DNA photolyases. The consensus sequence is presented at the bottom of the alignment, while conservation percentage has been deduced in the form of the line graph. Key: 8HDF-binding sites (arrow), MTHF-binding sites (broken vertical line), FAD-binding sites (horizontal bar), positive ring (arrow with rounded tip), and substrate-binding site (arrow with polygonal tip).

intriguingly, Gly242 of P3 was replaced by positively charged residues Arg236 and His232 in P1 and P2, respectively. Since reduced FAD (excited) is a negatively charged molecule (Carell et al. 2001; Sancar 2003), the presence of such positively charged residues at FAD-binding sites may intensify P1 and P2 association with their indispensable catalytic cofactor. A substitution at Ala385 of P3 and P2 with Asn 276 of P1 was also observed. However, the mentioned substitution was not involved significantly in the groove architecture of FAD-binding sites (this will be discussed later). Additionally, active-site residues (Glu266, Trp269, Asn332, Met336 and Trp275) were conserved in all under consideration photolyases. Similarly, Arg222, Arg333, Arg388 and Lys398 of P1, which develop the positively charged rim at or around the active site, were also found almost conserved at the corresponding positions of P2 and P3, except for Lys398, which was found replaced by Glu406 in P2 (Fig. 1). Since the positive rim around the substrate-binding site is stipulated as crucial for the interaction of the substrate (dimers) with the binding sites (Komori et al. 2001), the lack of positive residues in *E. coli* photolyase (P2) may adversely affect its efficacy as compared to photolyases of *E. faecalis* (P1) and *A. nidulans* (P3).

As mentioned earlier, class I photolyases have been further classified into two subtypes on the basis of their

LHC. In order to decipher the functional type of P1, the potential and/or known sites of MTHF in P2 (folate-type) and 8-HDF in P3 (deazaflavin-type) were compared with primary structure of P1. Interestingly, no MTHF-binding sites were noticed in P1, when compared with the sequence of P2. Conversely, most of the 8-HDF-binding sites, more specifically, Arg9, Phe35, Gln40, Asp98 and Gly103 were detected in P1 and P3. However, three iso-functional amino acid substitutions were observed (Fig. 1).

Holistically, some interesting inferences could be drawn from the sequence comparison. Firstly, the strong degree of conservation present in C-terminal of all sequences more precisely at FAD-binding sites, substrate-binding sites and positive rim defining regions suggest the indispensability of the residues in terms of catalytic activity of the enzyme. However, discrepancies present in the LHC-binding sites among the photolyases on the one hand categorized the enterococcal photolyase (P1) as deazaflavin-type similar to that found in *A. nidulans* (P3) and *Thermus thermophilus*, but it also implicates their dispensability among prokaryotic kingdom. Indeed, absence of LHC has not been found to affect the enzyme specificity towards substrate and neither its catalytic tendency. However, its presence may increase the catalytic rate by 10 to 100 fold (Sancar 2003). Moreover, presence of deazaflavin-type

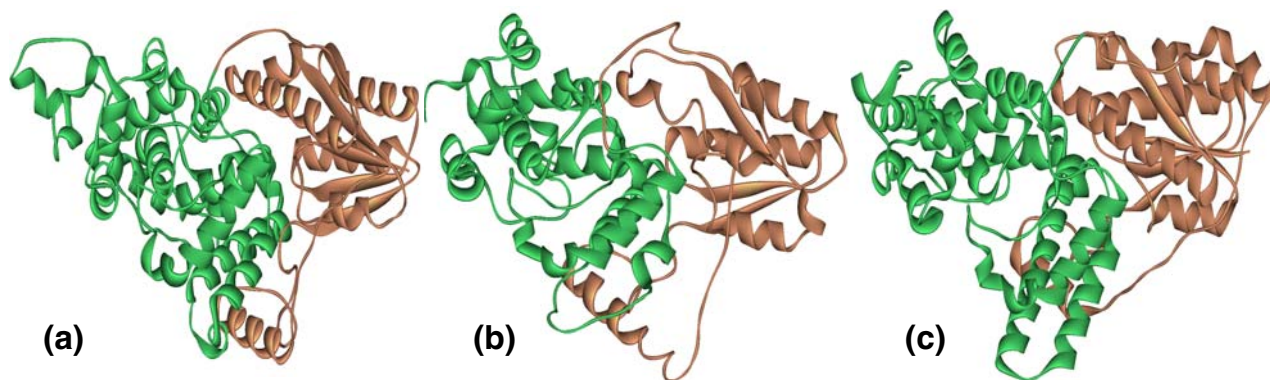


Fig. 2. Tertiary structure of photolyases. Tertiary structures (a) *E. coli* (P2), (b) *E. faecalis* (P1), and (c) *A. nidulans* (P3) share the same C α backbone structure with N-terminal (brown color) comprises on α/β domain, while C-terminal (green color) is made up of helical domain.

photolyase in *E. faecalis* implicates towards its ancient root as the similar type of photolyase have been isolated from the phylogenetically deep-rooted organisms (*A. nidulans*, *T. thermophilus*) (Tamada et al. 1997; Komori et al. 2001).

Overall structure

The three-dimensional model of enterococcal photolyase (P1) seemed to be relatively less structured than the crystal structures of both P2 and P3. However, similar to both structures (P2 and P3), enterococcal photolyase (P1) also comprised on N-terminal α/β domain and C-terminal helical domain. The α/β domain was made up of 6 β -strands ($\beta 1$ – $\beta 6$) and 5 α -helices ($\alpha 1$ – $\alpha 5$). Collectively, the domain was found composed of an open β -sheet structure with a typical dinucleotide binding fold as also been found in both understudy photolyases. Similarly, a long loop, which connects the N-terminal α/β domain with C-terminal helical domain, was also observed in P1 as in P2 and P3. Interestingly, in contrast to both P2 and P3 (Park et al 1995; Tamada et al 1997), an intervening β -sheet was found present in the loop of P1 (enterococcal photolyase), which may contribute to its structural stability. In comparison, the helical domain of enterococcal protein was less structured and borne 11 helices ($\alpha 6$ – $\alpha 17$), however, the number of 3_{10} -helices remained the same as three at almost corresponding position in comparison of P2 and P3. Moreover, C-terminal of P1 was found to end in an unstructured coil in contrast to other structured photolyases (P2 and P3) where the C-terminal ended in helical structure (Fig. 2). The rms deviation of *E. faecalis* photolyase was found as 0.37 Å and 0.72 Å for the overlaps with the photolyase of *A. nidulans* (template) and *E. coli*, respectively. The rms deviations not only suggest the fidelity of modeling approach but also indicate that consistency of the same C α backbone architecture in different types of photolyase.

FAD-binding sites

As discussed earlier, FAD (catalytic cofactor) is a common chromophore present in both folate- and

deazaflavin-type photolyases. Consistent with the sequence similarity, FAD-binding residues of *E. faecalis* photolyase were found at almost corresponding spatial positions and orientation with reference to both *A. nidulans* and *E. coli* photolyases (Park et al. 1995; Tamada et al. 1997). Precisely, based on binding residues it could be inferred here that FAD is deeply buried at the centre of four-helix bundle and accessible for electron exchange through the central hole in the surface of helical domain (Fig. 3). However, the diameter of the hole was found more similar in P1 and P3 (deazaflavin-type) than in P2 (folate-type) implying the role of neighboring residues in developing the difference at FAD-binding sites in deazaflavin-type photolyase. Overall, in all the compared photolyases, the groove appeared hydrophobic in nature that may favor the FAD-binding (unexcited and/or uncharged) to photolyases.

LHC-binding sites

From the multiple sequence alignment it was established that the LHC of enterococcal photolyase (P1) is 8-HDF, thus this photolyase is a deazaflavin-type photolyase (Fig. 1). Contrary to the conserved-binding position of FAD, 8-HDF (LHC of deazaflavin-type photolyase) binds at spatially different positions compared to MTHF (LHC of folate-type photolyase). Similarly, in P1 and P3, 8-HDF-binding sites were found interiorly situated in α/β domain, while the LHC-binding sites of P2 were exteriorly placed between α/β and helical domain (Fig. 3). Moreover, the electrostatic surface topology of the region unraveled that binding surfaces of 8-HDF in P1 and P3 were extremely narrow and more like a crevice, rather than groove as found in the case of MTHF-binding sites of P2 (Park et al. 1995; Tamada et al. 1997). Despite having different types of LHC and consequently their binding sites in folate- and deazaflavin-type of photolyases, all P1, P2 and P3 showed the same tertiary structures of α/β domain. Interestingly, there are very few examples in which homologous primary and tertiary structures of closely related enzymes interact with

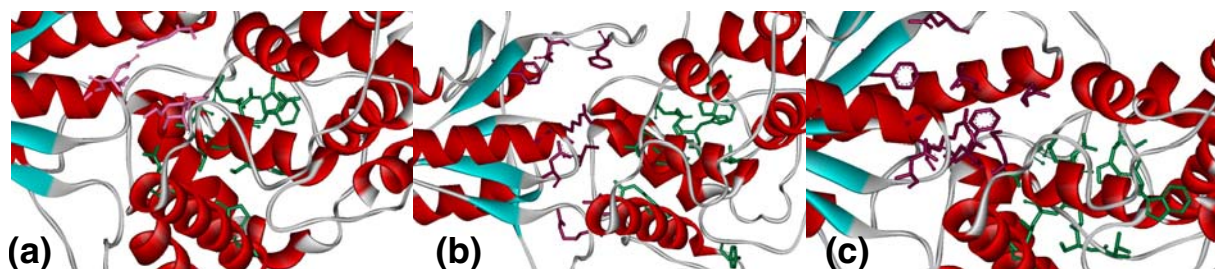


Fig. 3. Cofactors-binding sites of photolyases. Binding sites of catalytic cofactor FAD (green), light harvesting cofactor MTHF (pink) and 8-HDF (maroon) of (a) *E. coli*, (b) *E. faecalis*, and (c) *A. nidulans* photolyase. Note the orientation of FAD and 8-HDF in P1 (b) and P3 (c) towards each other in contrast to P2 (a), where the cofactor binding sites are exteriorly oriented.

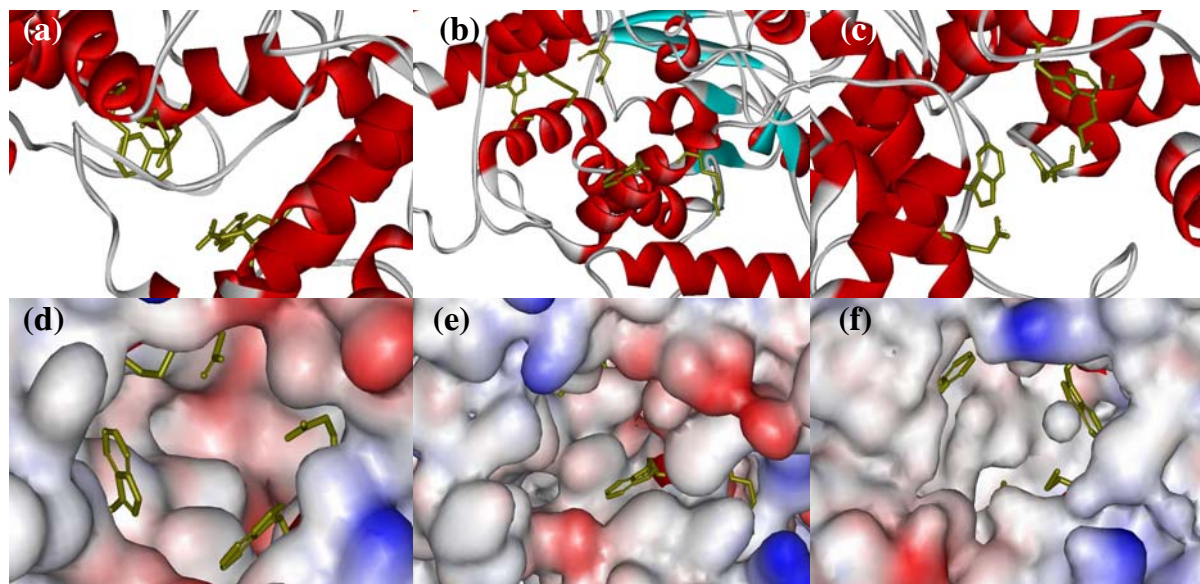


Fig. 4. Substrate-binding sites of photolyases. Substrate-binding sites (a) *E. coli* (P2), (b) *E. faecalis* (P1), and (c) *A. nidulans* (P3) are situated in the central helical region of the proteins. The electrostatic surface potential for *E. coli* (d), *E. faecalis* (e) and *A. nidulans* (f) shows the presence of more positive residues in *E. faecalis* and *A. nidulans*.

two different types of cofactor at spatially different places.

Interchromophoric energy transfer

Transfer of harvested energy from LHC to catalytic cofactor is essential for photolyase-mediated DNA repair. The average distance between LHC and FAD has been deduced as 17.5 Å in P2 and 16.8 Å in P3 (Park et al. 1995; Tamada et al. 1997). Moreover, time-resolved fluorescence experiments have shown that the efficiency of energy transfer is 98% and 62%, respectively, in P3 and P2 (Kim et al. 1991, 1992). As FAD- and 8-HDF-binding sites were found at the same place and orientation in P1 and P3, the similar inference of more efficient catalytic activity could be extended for enterococcal photolyase (P1) (Fig. 3). This notion has been further strengthened by the association of high efficiency of catalytic activity with the orientation of cofactor-binding sites (both LHC and catalytic cofactor) that favors the energy transfer between the two cofactors by long-range dipole-dipole interaction (Kim et al. 1991, 1992; Tamada et al. 1997). Taking these observations into account it is plausible to state that photolyase of *E. faecalis* may be more efficient in its catalytic activity

in comparison to its counterpart from *E. coli* rendering the more tolerance of *E. faecalis* to UV irradiation than *E. coli*.

Substrate-binding sites

Multiple sequence alignment clarified substantial conservancy among the substrate-binding sites of all photolyases, however, electrostatic surface potential revealed relatively narrow hole with more positively charged rim in deazaflavin-type photolyase (P1 and P3) as compared to its counterpart (folate-type; P2), which bore larger hole with less positive charges at the surface (Fig. 4). More specifically, it has been suggested that FAD (catalytic cofactor) becomes accessible to dimers through a positively charged concave surface hole and then transfers an electron in order to bring cleavage in dimers and restore the native form of the bases (Roberts et al. 1998; Komori et al. 2001). Taking this into account the present findings implies to more catalytic efficiency of the photolyase of *E. faecalis* in comparison to *E. coli* in correcting the CPDs.

Fold recognition

Expectedly, most of the folds present in *E. faecalis* pho-

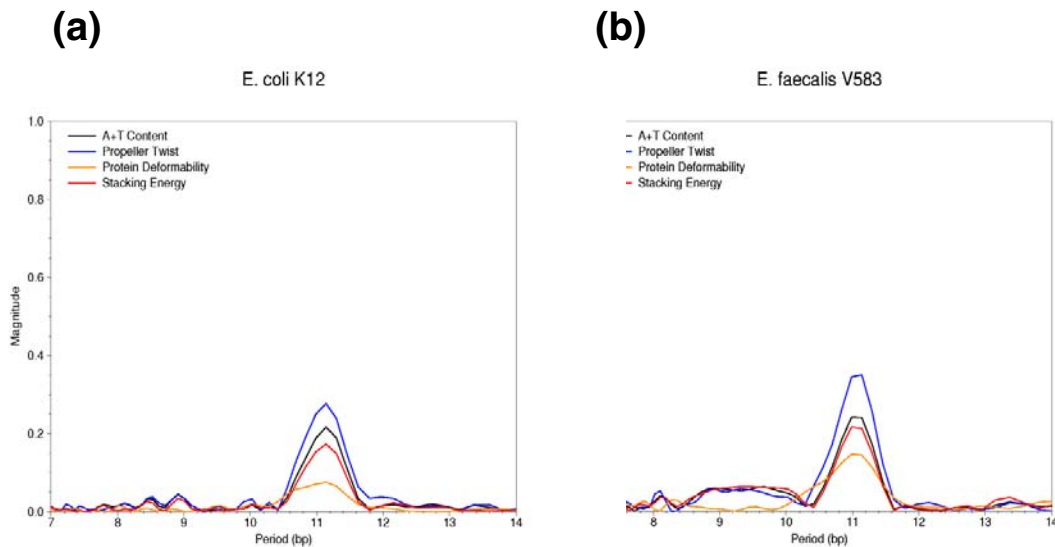


Fig. 5. Protein induced genomic deformability. Periodicity calculation as present on CBS (Hallin & Ussery 2004) indicates that *E. coli* genome (a) is more rigid than *E. faecalis* genome (b) upon interaction with protein. The graphs have been retrieved from CBS server (<http://www.cbs.dtu.dk/services/GenomeAtlas/>). Note the orange line represents the protein induced deformability in the respective genome.

tolyase were found similar to what is present in the either cryptochromes of *Synechocystis* spp. and other photolyases of different prokaryotes. However, despite very low protein identity (15%) some folds resembled with the folds of other DNA-binding proteins, like transcriptional regulators. Moreover, earlier studies have revealed that photolyases have a distant relationship with class I aminoacyl-tRNA synthetases and electron transport flavoproteins (Aravind et al. 2002).

Protein induced genomic deformability

Atomic protein force microscopy studies has revealed that on binding with photolyases DNA tends to bend at an angle of 36°; this may play some role in base flipping of the dimer (Berg et al. 1998; van Noort et al. 1999). In this connection we found that genome periodicities of *E. faecalis* V583 was higher than several sequenced genomes of *E. coli* in terms of protein induced deformability (Fig. 5) (Worning et al. 2001). The findings imply that beside the more efficient catalytic feature found in photolyase of enterococci, its genome is also more flexible than *E. coli* upon interaction with protein.

Conclusion

Conclusively, modeled structure of *E. faecalis* photolyase is considerably conserved with the crystal structures of *A. nidulans* and *E. coli*. Multiple sequence alignment has shown strong conservation of FAD- and substrate-binding sites in all the three photolyases. However, with reference to LHC-binding sites enterococcal photolyase is significantly similar to deazaflavin-type photolyase of *A. nidulans* at primary to tertiary structure level. Additionally, the orientation and placement of residues of the cofactors-binding sites also imply to the substantially efficient energy transfer in enterococcal photolyase than of *E. coli*. Genomic periodicities also implicate that genome of *E. faecalis* is

more responsive for the action of its photolyase than *E. coli*. Briefly, the findings suggest that DNA photolyase of *E. faecalis* is catalytically more active than *E. coli* photolyase; the greater catalytic activity may be translated in terms of low inactivation rate of *E. faecalis* than *E. coli*, therefore making it more suitable fecal contamination indicator. It is our belief that the present effort is first of its kind to explicate low sunlight inactivation rate of *Enterococcus* in terms of structure-function association of photolyase. We also realize that more studies towards substrate and cofactors docking with the protein may illustrate more insights in this regard. Such studies are underway and will be reported shortly.

References

- Altschul S.F., Madden T.L., Schäffer A.A., Zhang J. Zhang Z., Miller W. & Lipman D.J. 1997. Gapped BLAST and PSI-BLAST: a new generation of protein database search programs. *Nucleic Acids Res.* **25**: 3389–3402.
- Aravind L., Anantharaman V. & Koonin E.V. 2002. Monophyly of class I aminoacyl tRNA synthetase, USPA, E/TFP, photolyase, and PP-ATPase nucleotide-binding domains: Implications for protein evolution in the RNA world. *Proteins* **48**: 1–14.
- Bates P.A., Kelley L.A., MacCallum R.M. & Sternberg M.J.E. 2001. Enhancement of protein modelling by human intervention in applying the automatic programs 3D-JIGSAW and 3D-PSSM. *Proteins* **45** (Suppl. 5): 39–46.
- Berg B.J.V. & Sancar G.B. 1998. Evidence for dinucleotide flipping by DNA-photolyases. *J. Biol. Chem.* **273**: 20276–20284.
- Berman H.M., Westbrook J., Feng Z., Gililand G., Bhat T.N., Weissig H., Shindylaov I.N. & Bourne P.E. 2000. The Protein Data Bank. *Nucleic Acids Res.* **28**: 1235–1242.
- Carell T., Burgdorf L.T., Kundu L.M. & Cichon M. 2001. The mechanism of action of DNA photolyases. *Curr. Opin. Chem. Biol.* **5**: 491–498.
- Cashmore A.R., Jarillo J.A., Wu Y.J. & Liu D. 1999. Cryptochromes: blue light receptors for plants and animals. *Science* **284**: 760–765.

- Clingen P.H., Arlett C.F., Roza L., Mori T., Nikaido O. & Green M.H.L. 1995. Induction of cyclobutane pyrimidine dimers, pyrimidine (6–4) pyrimidine photoproducts, and Dewar valence isomers by natural sunlight in normal human mononuclear cells. *Cancer Res.* **55**: 2245–2248.
- Davies-Colley R.J., Bell R.G. & Donnison A.M. 1994. Sunlight inactivation of enterococci and fecal coliforms within sewage effluent diluted in seawater. *Appl. Environ. Microbiol.* **60**: 2049–2058.
- Eker A.P.M., Koolman P., Hessels J.K.C. & Yasui A. 1990. DNA photoreactivating enzyme from the cyanobacterium *Anacystis nidulans*. *J. Biol. Chem.* **265**: 8009–8015.
- Eisenberg D., Luthy R. & Bowie J.U. 1997. VERIFY3D: assessment of protein models with three-dimensional profiles. *Methods Enzymol.* **277**: 396–404.
- Epple R. & Carell T. 1998. Flavin and deazaflavin containing mode, compounds mimic the energy-transfer step in type II DNA photolyases. *Angew. Chem. Int. Ed. Engl.* **37**: 938–941.
- Guex N. & Peitsch M.C. 1997. SWISS-MODEL and the Swiss-PdbViewer: an environment for comparative protein modeling. *Electrophoresis* **18**: 2714–2723.
- Hallin P.F. & Ussery D.W. 2004. CBS Genome Atlas Database: a dynamic storage for bioinformatic results and sequence data. *Bioinformatics* **20**: 3682–3686.
- Harrison C.B., O’Neil L.L.O. & Wiest O. 2005. Computational studies of DNA photolyase. *J. Phys. Chem.* **109**: 7001–7012.
- Hussain M., Rassol S.A., Khan M.T. & Wajid A. 2007. Enterococci vs. coliforms as a possible fecal contamination indicator: baseline data for Karachi. *Pak. J. Pharm. Sci.* **20**: 107–111.
- Johnson J.L., Hamm-Alvarez S., Payne G., Sancar G.B., Rajagopalan K.V. & Sancar A. 1988. Identification of second chromophore of *Escherichia coli* and yeast DNA photolyase as 5,10-methenyltetrahydrofolate. *Proc. Natl. Acad. Sci. USA* **85**: 2046–2050.
- Kato R., Hasegawa K., Hidaka Y., Kuramitsu S. & Hoshino T. 1997. Characterization of a thermostable DNA photolyase from an extremely thermophilic bacterium, *Thermus thermophilus* HB27. *J. Bacteriol.* **179**: 6499–6503.
- Kelley L.A., MacCallum R.M. & Sternberg M.J.E. 2000. Enhanced genome annotation using structural profiles in the program 3D-PSSM. *J. Mol. Biol.* **299**: 499–520.
- Kim S.T., Heelis P.F., Okamura T., Hirata Y., Mataga N. & Sancar A. 1991. Determination of rates and yields of interchromophore (folate-flavin) energy transfer and intermolecular (flavin-DNA) electron transfer in *Escherichia coli* photolyase by time-resolved fluorescence and absorption spectroscopy. *Biochemistry* **30**: 1126–11270.
- Kim S.T., Heelis P.F. & Sancar A. 1992. Energy transfer (deazaflavin→FADH₂) and electron transfer (FADH₂→T<>T) in *Anacystis nidulans* photolyase. *Biochemistry* **31**: 11244–11248.
- Komori H., Masui R., Kuramitsu S., Yokoyama S., Shibata T., Inoue Y. & Miki K. 2001. Crystal structure of thermostable DNA photolyase: pyrimidine-dimer recognition mechanism. *Proc. Natl. Acad. Sci. USA* **98**: 13560–13565.
- Laskowski M.J. & Kato L. 1980. PROCHECK. *Annu. Rev. Biochem.* **49**: 593–626.
- Melo F. & Feytmans E. 1998. Assessing protein structures with a non-local atomic interaction energy. *J. Mol. Biol.* **277**: 1141–1152.
- Nicholas K.B., Nicholas Jr. H.B. & Deerfield II D.W. 1997. GeneDoc: Analysis and Visualization of Genetic Variation. *EMBL-Net News* **4**: 1–4.
- Park H.W., Kim S.T., Sancar A. & Deisenhofer J. 1995. Crystal structure of DNA photolyase from *Escherichia coli*. *Science* **268**: 1866–1872.
- Roberts R.J. & Cheng X. 1998. Base flipping. *Annu. Rev. Biochem.* **67**: 181–198.
- Sancar A. 2003. Structure and function of DNA photolyase and cryptochrome blue light photoreceptors. *Chem. Rev.* **103**: 2203–2238.
- Schwede T., Kopp J., Guex N. & Peitsch M.C. 2003. SWISS-MODEL: an automated protein homology-modeling server. *Nucleic Acids Res.* **31**: 3381–3385.
- Sinton L.W., Finlay R.K. & Lynch P.A. 1999. Sunlight inactivation of fecal bacteriophages and bacteria in sewage polluted seawater. *Appl. Environ. Microbiol.* **68**: 1122–1131.
- Sinton L.W., Hall C.H., Lynch P.A. & Davies-Colley R.J. 2002. Sunlight inactivation of fecal indicator bacteria and bacteriophages and bacterial indicators in Moselle river (France). *Water Res.* **36**: 3629–3637.
- Tamada T., Kitadokoro K., Higuchi Y., Inaka K., Yasui A., de Ruiter P.E., Eker A.P. & Miki K. 1997. Crystal structure of DNA photolyase from *Anacystis nidulans*. *Nat. Struct. Biol.* **4**: 887–891.
- Thomson C.L. & Sancar A. 2002. Photolyase/cryptochrome blue-light photoreceptors use photon energy repair DNA and reset the circadian clock. *Oncogene* **21**: 9043–9056.
- Thompson J.D., Gibson T.J., Plewniak F., Jeanmougin F. & Higgins D.G. 1997. The Clustal X windows interface: flexible strategies for multiple sequence alignment aided by quality analysis tools. *Nucleic Acids Res.* **25**: 4876–4882.
- van Noort S.J.T., Orsini F., Eker A.P.M., Wyman C., de Grooth B. & Greve J. 1999. DNA bending by photolyase in specific and non-specific complexes studied by atomic force microscopy. *Nucleic Acids Res.* **27**: 3875–3880.
- Wheeler D.L., Barrett T., Benson D.A., Bryant S.H., Canese K., Church D.M., DiCuccio M., Edgar R., Federhen S., Helmberg W., Kenton D.L., Khovayko O., Lipman D.J., Madden T.L., Maglott D.R., Ostell J., Pontius J.U., Pruitt K.D., Schuler G.D., Schriml L.M., Sequeira E., Sherry S.T., Sirotkin K., Starchenko G., Suzek T.O., Tatusov R., Tatusova T.A., Wagner L. & Yaschenko E. 2005. Database resources of the National Center for Biotechnology Information. *Nucleic Acids Res.* **33** (Database Issue): 39–45.
- Worning P., Jensen L.J., Nelson K.E., Brunak S. & Ussery D.W. 2000. Structural analysis of DNA sequences: evidence for lateral gene transfer in *Thermotoga maritima*. *Nucleic Acids Res.* **28**: 706–709.
- Yasui A., Eker A.P., Yshuira S., Yajima H., Kobayashi T., Takao M. & Oikawa A. 1994. A new class of DNA photolyases present in many organisms including aplacental mammals. *EMBO J.* **13**: 6143–6151.
- Yoon J.H., Lee C.S., Oconnor T.R., Yasui A. & Pfeifer G.P. 2000. The DNA damage spectrum produced by simulated sunlight. *J. Mol. Biol.* **299**: 681–693.
- Zhong D. 2007. Ultra fast catalytic processes in enzymes. *Curr. Opin. Chem. Biol.* **11**: 174–181.

Received December 29, 2008

Accepted May 27, 2009